

# CCQ: Convolutional Code for Extreme Low-bit Quantization in LLMs

Zhaojing Zhou, Xunchao Li, Minghao Li, Handi Zhang, Haoshuang Wang, Wenbin Chang, Yiqun Liu, Qingqing Dang, Dianhai Yu, Yanjun Ma, Haifeng Wang

Baidu Inc.

## Abstract

The rapid scaling of Large Language Models (LLMs) elevates inference costs and compounds substantial deployment barriers. While quantization to 8 or 4 bits mitigates this, sub-3-bit methods face severe accuracy, scalability, and efficiency degradation. We propose Convolutional Code Quantization(CCQ), an inference-optimized quantization approach compressing LLMs to 2.0–2.75 bits with minimal accuracy loss. Departing from error-prone scalar quantization or slow vector quantization, CCQ integrates a hardware-aware bit-shift encoding and decoding solution with Convolutional Code, Hybrid Encoding, and Code Cluster, jointly overcoming accuracy-speed bottlenecks. We construct a lookup-free encoding space, enabling a linear mapping between the codebook and weight vectors, thereby optimizing inference performance. Meanwhile, by drawing on the concept of data mapping from vector quantization, we minimize the performance degradation of the model under extremely low-bit conditions. Experiments demonstrate that CCQ achieves outstanding performance on LLMs across various benchmarks. We compress DeepSeek-V3(671B total parameters) to 184GB and ERNIE-4.5-300B-A47B to 89GB, enabling single-GPU deployment of ERNIE 4.5 and eliminating inter-card communication. The 2-bit ERNIE-4.5-300B-A47B model and inference engine have been open-sourced.

## 1 Introduction

Large Language Models(LLMs) demonstrate state-of-the-art capabilities across artificial intelligence domains, spanning natural language processing to multi-modal understanding. However, these performance gains coincide with significant inference degradation, impeding cost-effective large-scale deployment. Contemporary flagship models exemplify this scalability challenge: Qwen2 (Yang et al., 2024a), Qwen2.5 (Yang et al., 2024b), and

Llama 3 (Grattafiori et al., 2024) series have around 100 billion parameters within their most powerful members. The emergence of Mixture-of-Experts (MoE) architecture further escalates model scale—evidenced by Llama 3.1 (405B) (Grattafiori et al., 2024), DeepSeek-V3 (671B) (DeepSeek-AI et al., 2025), Qwen3 (235B) (Yang et al., 2025), and ERNIE 4.5 (300B / 424B) (Baidu-ERNIE-Team, 2025). Such massive parameterization exacerbates inference latency, primarily due to memory constraints and cross-device communication overhead in distributed environments.

Quantization (Gray and Neuhoff, 1998), a cornerstone technique for model compression and efficient deployment, reduces parameter precision from 16 bits to 8 or 4 bits, yielding more than 50% memory savings. Common quantization configurations include Weight-Only Quantization(WOQ) (Frantar et al., 2022; Lin et al., 2024), Weight-Activation Quantization(WAQ) (Xiao et al., 2023) and KV Cache Quantization(KVQ) (Liu et al., 2024c; Hooper et al., 2024). WOQ and KVQ primarily alleviate memory bottlenecks—critical for models with massive parameter counts or long context windows—by compressing weights and key-value caches. WAQ, conversely, exploits hardware acceleration for low-precision matrix operations (e.g., INT8/FP8) to achieve compute-bound speedups.

Recent efforts pursue extremely low-bit quantization (e.g., 2 bits) to further reduce LLM deployment costs. However, these methods invariably compromise either model accuracy or inference efficiency, limiting their practical utility. Post-training quantization (PTQ) algorithms like GPTQ (Frantar et al., 2022) and AWQ (Lin et al., 2024) use scalar quantization to convert weights to low-bit integers. While effective at 4 bits by smoothing outliers, they typically fail at 2 bits due to the constrained numerical space.

In contrast, vector quantization (van Baalen et al.,

2024; Liu et al., 2024b; Tseng et al., 2024a; Malinovskii et al., 2024) aims for higher compression and better performance by representing weights as indices into a finite codebook of high-precision vectors. During quantization, weights are clustered and replaced by codebook indices; storage is compressed by saving these indices and the codebook. Inference reconstructs weights via codebook lookup.

Despite offering superior compression fidelity over scalar quantization, vector quantization introduces critical performance bottlenecks. The dequantization process requires large-scale, non-contiguous codebook lookups based on indices. This irregular memory access pattern violates data locality, prevents efficient hardware utilization, causes pipeline stalls, and introduces latency proportional to codebook size, severely degrading LLM inference throughput.

To circumvent the performance drawbacks associated with inference-unfriendly codebooks while preserving the benefits of mapping high-dimensional vectors to low-dimensional vectors in vector quantization, we propose convolutional code quantization by integrating convolutional encoding with scalar quantization. By combining innovative hybrid encoding and code cluster, we achieve several extremely low-bit quantization configurations. Initially, we construct a codebook based on convolutional codes, leveraging their inherent properties to achieve efficient bitshift decoding. Subsequently, we employ scalar quantization to establish a linear mapping between high-dimensional and low-dimensional vectors. This approach not only obviates the need for storing a codebook but also replaces time-consuming indexing operations with linear computations, thereby offering both performance and efficacy benefits. Our main contributions are as below:

- **Convolutional Code Quantization (CCQ):** We propose a novel weight-only PTQ solution for extreme compression of LLMs. By integrating convolutional coding theory, hybrid encoding, and code cluster algorithms, CCQ achieves around 70% model size savings at 2-bit precision compared with 8-bit counterpart, while maintaining near-lossless accuracy on both DeepSeek-V3 and ERNIE 4.5 models.
- **Bit-Shift Decoding Inference:** Our co-designed bit-shift decoding strategy establishes inference latency similar to scalar-based

quantization. This enables unprecedented deployment of ERNIE-4.5-300B-A47B (the largest ERNIE 4.5 language model) on a single NVIDIA H20 GPU without intra-node communication overhead.

- **Open-Source:** We publicly release 2-bit quantized ERNIE 4.5 variants<sup>1</sup> with around 2% accuracy degradation relative to baselines. The inference code is available at <https://github.com/PaddlePaddle/FastDeploy/tree/develop>.

## 2 Background and Related Work

### 2.1 Scalar-based Quantization

RTN (Round-to-Nearest) is the most straightforward method for quantizing weight and activations by using the min-max values calibrated from a dataset. However, the quantization error increases significantly when the number of bits is small, especially when significant outliers exist. GPTQ (Frantar et al., 2022) updates the weight values based on the previous quantization error and the inverse of the Hessian matrix calculated from the activations. AWQ (Lin et al., 2024) transferred outliers from weights to activations to smooth the distributions. Group-wise quantization is applied to both methods. However, these methods still suffer from non-negligible accuracy degradation even under 3/4-bit quantization, primarily constrained by the limited dynamic range of integer representation.

SqueezeLLM (Kim et al., 2023) implements non-uniform quantization and Hessian Metrics, GPTAQ (Li et al., 2025) explicitly minimizes the quantization error as well as the accumulated asymmetry error for better performance under low-bit quantization. HQQ (Badri and Shaji, 2023) and HQQ+ (Badri and Shaji, 2024) introduce Hyper-Laplacian distribution to better capture the heavy-tailed outlier errors compared to MSE. However, substantial performance degradation still exists for 2 bits and even lower bits.

To improve the extremely low-bit model performance, Quantization-Aware-Training (QAT) is introduced in recent works. LLM-QAT (Liu et al., 2023) achieves 4 bits on weights and KV Cache. But distillation is required to maintain the accuracy, which leads to heavy training pipelines. Bit-Net (Wang et al., 2023) achieves 1.58-bit quantization by introducing QAT from the pre-training

<sup>1</sup><https://huggingface.co/baidu/ERNIE-4.5-300B-A47B-2Bits-Paddle>

phase. However, the prolonged training duration and inherently limited scalability significantly constrain their practical deployment. OneBit (Xu et al., 2024) and LittleBit (Lee et al., 2025) attempt to combine matrix decomposition and QAT for higher compression ratios. However, they still fail to eliminate the quantization cost and training instability.

## 2.2 Vector-based Quantization

To overcome the performance limit of scalar-based quantization, vector-based quantization methods are introduced for low-bit quantization.

Vector Quantization (Gray, 1984) (VQ) is originally designed for lossy data compression. It works by categorizing a large set of vectors into a small one based on some clustering algorithms, like K-means. In the LLMs, index maps and codebooks are stored as the compressed weights to achieve the extreme compression ratio.

The main problem for VQ is how to balance the accuracy and its quantization cost. AQLM (Egiazarian et al., 2024; Malinovskii et al., 2024) attempts to maximize the codebook’s dimensionality, leaving the unstructured indexing the main bottleneck for inference speed. QUIP# (Tseng et al., 2024a) uses incoherence processing and E8 lattice for smaller codebook size, but it induces post-processing for Random Hadamard Transform (RHT), which hurts inference speed as well. VPTQ (Liu et al., 2024b) parallelly updates the vector in one column to avoid error accumulation and introduces residual quantizations for higher accuracy. However, it also falls short in improving inference performance.

## 2.3 Convolutional Code

Convolutional codes represent a classic technique in channel coding, which involves continuous encoding of each state within the channel. Their primary characteristic lies in preserving the memory effect of the channel, where each current state’s code value is derived from the transition of the preceding state.

Fischer et al. (Marcellin and Fischer, 1990) applied a representation of convolutional codes known as trellis codes to quantization, thereby introducing Trellis-Coded Quantization (TCQ). Subsequently, QTIP (Tseng et al., 2024b) further enhances TCQ in terms of memory usage and decoding speed. Firstly, QTIP employs incoherent processing to transform weights into an independent Gaussian-like source, which is well-suited

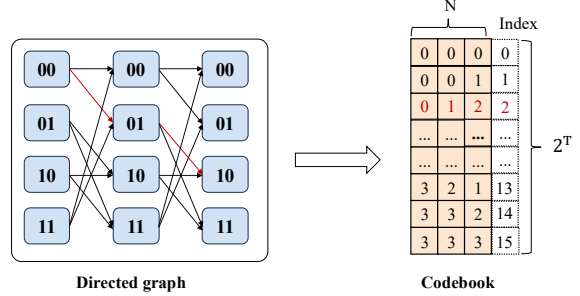


Figure 1: Convolutional code codebook construction. Taking ( $L=2$ ,  $N=3$ ,  $S=1$ ) configuration as an example, all the connection relationships among states in the directed graph are consolidated into a codebook. In the codebook, each row represents  $N$  consecutive states, and the corresponding convolutional code is the index.

for the trellis code. Secondly, the researchers devised computation-based pseudo-Gaussian codes to circumvent the need for storing codebooks and defining network architectures. Despite achieving favorable outcomes, QTIP still suffers from the drawback of computational complexity.

## 3 Methodology

This section presents the core elements of our proposed method. Firstly, in Section 3.1, we will elaborate on how we integrate convolutional codes with scalar quantization to construct a codebook capable of achieving linear mapping between high-dimensional and low-dimensional vectors, along with an overview of the framework of our algorithms. Subsequently, in Section 3.2, we demonstrate how we flexibly combine different convolutional codes to attain a higher compression ratio through hybrid encoding. Furthermore, in Section 3.3, we transcend the limitations imposed by data types in encoding and storage by employing the code cluster, thereby achieving significantly superior compression performance. In Section 3.4, we introduce the implementation details of scale compression and optimization. In Section 3.5, we present the performance optimization in the inference implementation.

### 3.1 Convolutional Code Quantization

Unlike TCQ and QTIP, which perform sequential encoding on long sequences, we employ a vector-quantization-like approach to compress weights into vector groups. By simplifying the design of the codebook, we aim to reduce computational complexity during the encoding process. Consequently, we redefine convolutional codes from a directed

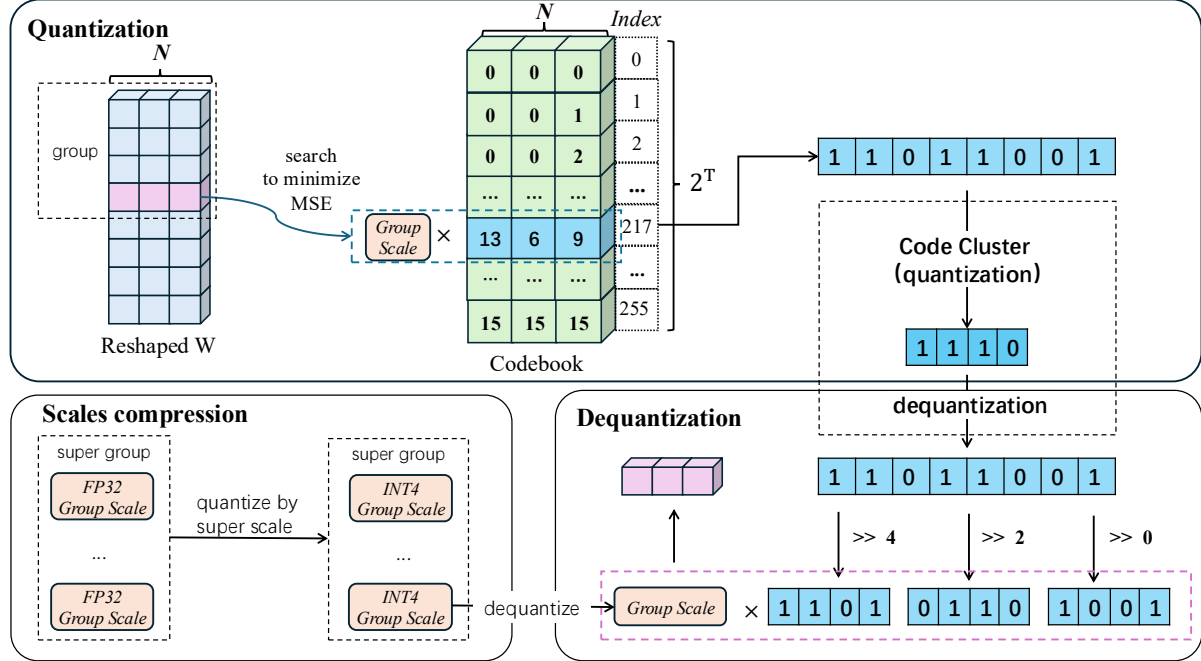


Figure 2: A schematic diagram of the CCQ. The dequantization part only involves shifting and dequantization calculations, and does not require the storage of a codebook. For the sake of simplicity, the codebook depicted in the figure is an example with parameters ( $L=4, N=3, S=2$ ). In reality, as mentioned in Section 3.3, we perform the code cluster under the configuration of  $(L=6, N=4, S=3)$ . The figure merely serves as an illustrative example.

graph representation to a finite set of vectors (i.e., the codebook).

#### Definition of Convolutional Code Codebook.

We define a convolutional encoding configuration as the triplet  $(L, N, S)$ , where  $L$  denotes the number of bits required for each state,  $N$  represents the number of states involved in a single encoding operation, and  $S$  indicates the number of transition bits between adjacent states. Here we define transition bits as the bits that do not overlap with the previous state. Figure 1 depicts all possible transition forms between adjacent states for the configuration  $(L=2, N=3, S=1)$ . Each state requires  $L = 2$  bits for representation. The transition between adjacent states is achieved using  $S = 1$  transfer bit to update the state. Consequently, there are  $L - S = 1$  redundant bits between adjacent states. Given the overlapping bits between adjacent states, after applying convolutional coding, we only need to store the code symbols of the initial state along with the state transition bits to fully represent the entire state sequence. For instance, considering the three states connected by the red line in Figure 1 ( $00 \rightarrow 01 \rightarrow 10$ ), the final stored code would be 0010. These three state values can then be placed in the index 2 (0010) of the codebook. Following this approach, we successfully transform the directed

graph into a code table comprising a collection of vectors, each of length  $N$ .

Evidently, for a given encoding configuration, the total number of bits in a set of convolutional codes is calculated as  $T = L + (N - 1) * S$ . Subsequently, we can generate a corresponding codebook  $\mathbf{C} \in \mathbb{Z}^{2^T \times N}$ .

Taking 4-bit quantization as an example in weight quantization, where each quantized weight requires 4 bits for storage, in the case of convolutional encoding with parameters set as  $(L=4, N=3, S=2)$ , we can store three quantized values using only 8 bits, achieving an equivalent compression effect of 2.66 bits per weight (bpw). Compared to the 4-bit weight quantization, this results in a 33% improvement in compression rate while maintaining the equivalent numerical precision as 4-bit quantization.

**Bitshift Decoding.** Due to the repetitive nature between adjacent states in convolutional codes, we can rapidly decode convolutional codes through bit shifting. Consequently, within the framework of convolutional code quantization, the dequantization process only involves bit-shifting operations and dequantization calculations for scalar quantization, which undoubtedly facilitates inference implementation more than index lookup in vector

quantization. The specific decoding process can be referred to in Figure 2.

**Group-wise Quantization.** Although the memory characteristic of convolutional codes offers convenience in storage and decoding, it also restricts the non-coherence of quantized weights. When weights contain a significant number of outliers, the coherence of quantized values diminishes, which is detrimental to convolutional coding. Therefore, we introduce group-wise quantization to mitigate the impact of outliers. The quantization granularity at the group-wise level not only ensures the quantization precision of scalar quantization but also reduces the encoding loss during convolutional coding. In scenarios where the group size is not a multiple of  $N$ , we will pad each group with zeros to fulfill the encoding requirements. This approach will not compromise the accuracy of quantization.

**The Overall Quantization Algorithm.** The complete process of the convolutional code quantization method is demonstrated in Algorithm 1. Firstly, we group the weights and calculate the quantization parameters for each group. Subsequently, we generate the encoding space based on the convolutional code configuration (at this stage, the codebook contains numerical values within the integer domain, denoted as  $\mathbf{C} \in \mathbb{Z}^{2^T \times N}$ ). We then transform these values into the same floating-point domain as the original weights using the group scale (resulting in  $\mathbf{C} \in \mathbb{R}^{2^T \times N}$ ). Finally, we compute the Mean Squared Error (MSE) loss between each weight and every vector in the codebook. The optimal code value is determined by searching for the one that yields the minimum MSE loss.

It is important to note that there is no need to store the actual vector values obtained from the search—only their corresponding indices need to be retained. The step is consistent with vector quantization, but the key difference lies in the fact that our method does not require storing a large codebook to maintain the mapping between indices and vectors.

In our convolutional encoding quantization scheme, the indices obtained from the search directly represent the final convolutional code values. During subsequent dequantization, the true quantized values can be retrieved through bit-shifting operations, and the original weights can be reconstructed via dequantization computations.

---

### Algorithm 1: Convolutional Code Quantization

---

```

Input :  $\mathbf{W} \in \mathbb{R}^{d_o \times d_i}$ : Original Weight
          $g$ : group size
          $(L, N, S)$ : Encoding configuration
Output :  $\mathbf{W}_q \in \mathbb{Z}$ : Weight with Convolutional Code

 $\mathbf{W}_g \leftarrow \text{Reshape } \mathbf{W} ; \quad // \mathbf{W}_g \in \mathbb{R}^{\frac{d_o \times d_i}{g} \times \frac{g}{N} \times N}$ 
 $\text{group scale} \leftarrow \mathbf{W}_g ; \quad // \text{group scale} \in \mathbb{R}^{\frac{d_o \times d_i}{g}}$ 
 $\mathbf{C} = \text{Construct\_codebook}(L, N, S) ;$ 
 $// \mathbf{C} \in \mathbb{Z}^{2^T \times N}$ 
 $\mathbf{C} = \mathbf{C} \times \text{group scale} ; \quad // \mathbf{C} \in \mathbb{R}^{\frac{d_o \times d_i}{g} \times 2^T \times N}$ 
 $\text{Indices} \leftarrow \arg \min_{i \in 2^T} \|\mathbf{v} - \mathbf{C}_i\|^2, \forall \mathbf{v} \in \mathbf{W}_g$ 
 $\mathbf{W}_q \leftarrow \text{Reshape Indices}$ 

```

---

## 3.2 Hybrid Encoding

Although our method can achieve arbitrary compression rates by adjusting the encoding configuration, the actual storage compression effect can only be realized when the code aligns with practical data types. Specifically, the storage bits for convolutional coding must be exact multiples of 8 to be stored using data types such as INT8 or INT16. However, achieving a high compression rate typically necessitates an increase in the number of encoding states. Due to the inherent correlation in convolutional coding, an excessive number of encoding states can significantly exacerbate precision loss. Therefore, to attain a higher compression rate, we propose the concept of hybrid encoding. Within a single group, multiple distinct encoding configurations are employed in a hybrid manner to meet storage requirements. Through meticulous design, we successfully alternate between the  $(L=3, N=3, S=2)$  and  $(L=3, N=4, S=2)$  configurations, encoding seven numerical values into 16 bits, ultimately achieving an equivalent bit rate of 2.28 bpw.

## 3.3 Code Cluster

By employing hybrid encoding, we can alleviate the constraints imposed by storage data types, but achieving further compression remains challenging. To realize true 2-bit weight quantization, we innovatively propose the code cluster algorithm that entirely breaks free from the limitations of encoding configurations on compression rates.

Our convolutional code quantization is conducted at a group-wise granularity. Given the vast encoding space, the encoding values utilized on each channel are quite limited. This observation raises the question: can we retain only the fre-

quently used encoding values and eliminate the redundant ones, thereby enhancing the overall compression rate by reducing the encoding space? Naturally, the idea of clustering comes to mind to distill the significant encoding values. However, clustering is a nonlinear operation, and its data reconstruction process inevitably requires index lookups.

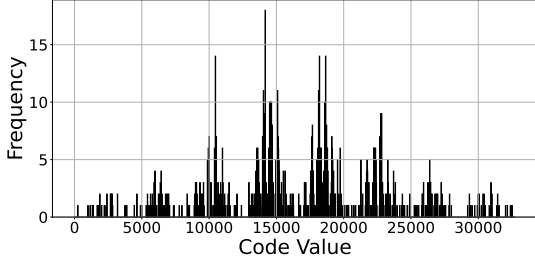


Figure 3: The code value distribution diagram of convolutional coding quantization on an output channel under the configuration of ( $L=6$ ,  $N=4$ ,  $N=3$ ).

Upon examining the numerical distribution of convolutional encoding quantization (Figure 3), we observe that the convolutional codes on each channel approximately follow a normal distribution, which is suitable for uniform quantization. Consequently, we propose utilizing uniform quantization to accomplish the code cluster, mapping any arbitrary encoding space into an 8-bit numerical range. As a result, all data reconstruction operations can be accomplished through computation. The computational formula for the code cluster is presented as follows:

$$\mathbf{C}' = \mathcal{Q}(\mathbf{C}) = \left\lfloor \frac{\mathbf{C} - \beta}{\alpha} \right\rfloor \quad (1)$$

where  $\mathbf{C} \in [0, 2^T - 1]$ ,  $\mathbf{C}' \in [0, 255]$ ,  $\alpha$  means code scale and  $\beta$  means code zero-point in asymmetric quantization.

Specifically, we first perform convolutional code quantization with parameters ( $L=6$ ,  $N=4$ ,  $S=3$ ) on the weights of each group. Subsequently, we conduct clusters of the code values along the dimension of output channels and map them to an 8-bit numerical range. This approach enables the storage of four parameters using only `UINT8`, achieving an equivalent compression effect of 2 bpw.

At this point, although the code cluster restricts the encoding space, the true quantized value of the weights is 6 bits. When combined with the group-wise quantization granularity, it can effectively ensure the numerical precision of critical

weights. Consequently, the impact on the model's performance is negligible.

### 3.4 Scale Optimization and Compression

**Scale Optimization:** After determining the encoded values through coding search, we can compute the quantization loss by dequantizing these values and comparing them with the original weights. The quantization error formula for a group of weight is as follows:

$$\begin{aligned} \text{Error} &= \sum_{i=0}^{g-1} \|\mathbf{W}_i - \mathcal{D}\mathcal{Q}(\mathbf{W}_i^q)\|^2 \\ &= \sum_{i=0}^{g-1} \|\mathbf{W}_i - \mathbf{W}_i^q \cdot S\|^2 \end{aligned} \quad (2)$$

where  $\mathbf{W}$  represents the original weight of a group,  $\mathbf{W}_q$  denotes the corresponding quantized values,  $g$  denotes the group size,  $\mathcal{D}\mathcal{Q}$  signifies the dequantization function, and  $S$  stands for the scale. For the sake of simplifying calculations, we directly use the decoded values to compute the quantization error, as bitshift decoding does not affect the accuracy of the quantized values.

At this stage, the scale  $S$  can be regarded as the sole variable. We can further reduce the quantization loss by updating the scale.

$$\frac{d\text{Error}}{dS} = 2 \sum_{i=0}^g (\mathbf{W}_i^q)^2 S - 2 \sum_{i=0}^g (\mathbf{W}_i \mathbf{W}_i^q) \quad (3)$$

By taking the derivative of the scale and setting  $\frac{d\text{Error}}{dS}$  to zero, we can determine the minimum value of the current loss.

$$S = \frac{\sum_{i=0}^{g-1} \mathbf{W}_i \cdot \mathbf{W}_i^q}{\sum_{i=0}^{g-1} (\mathbf{W}_i^q)^2} \quad (4)$$

**Scale Compression:** In the group-wise quantization, each group has its own scale factor. As the number of groups increases, the storage overhead associated with these scale factors becomes non-negligible. To address this, we propose quantizing the scale factors by channel-wise super scales and storing them in a low-bit format. Additionally, we observe that for the aforementioned 2.66 bpw (with  $L=4$ ,  $N=3$ ,  $S=2$ ) and the hybrid encoding scheme yielding 2.28 bpw, the group size is not divisible by the number of encoding states  $N$ . Consequently, the last code value in each group introduces redundant bits. Taking a group size of 64 as an example, under the ( $L=4$ ,  $N=3$ ,  $S=2$ ) configuration, 22 code

values are required to encode 64 parameters. In this scenario, only the first 4 bits of the last code value are valid, while the remaining 4 bits are redundant and need to be discarded after decoding. We can leverage these 4 redundant bits to store the quantized scale factor, ultimately achieving an equivalent bpw of 2.75. Similarly, for the hybrid encoding scheme with 2.28 bpw, 10 code values are necessary to encode 64 parameters, leaving 13 redundant bits that can be utilized to store the quantized scale factor, resulting in an equivalent bpw of 2.5. When it comes to the code cluster, redundant bits cannot be utilized, and additional consideration must be given to the storage overhead of the scale. For the code cluster of (L=6, N=4, S=3), the equivalent bit width is 2.06 bpw. The formula for calculating the equivalent bit width is presented below:

$$bpw = \begin{cases} \frac{T * \lceil \frac{g}{N} \rceil}{g}, & \text{if } g \equiv 1 \pmod{N} \\ \frac{T * \frac{g}{N}}{g} + \frac{\text{scale\_bits}}{g}, & \text{if } g \equiv 0 \pmod{N} \end{cases} \quad (5)$$

where  $T$  represents the total number of bits for a set of convolutional codes. However, when the code cluster is used,  $T$  denotes the number of bits required for the quantized code values, specifically  $T = 8$ .

### 3.5 Dequantization

In this section, we present the detailed implementation strategies for dequantizing weights within individual groups, as outlined in Algo. 2 and Algo. 3, and summarize the corresponding configurations in Table 1.

Table 1: Dequantization configuration for different encoding strategies.

(L,N,S)	bpw	Weight Mask	Scale Mask	Weight Bit-Shift	Code Cluster
(4,3,2)	2.75	0xF	0xF	[4,2,0]	No
(3,3,2)(3,4,2)	2.5	0x7	0x1FFF	[13,11,9,6,4,2,0]	No
(6,4,3)	2.06	0x3F	0xF	[9,6,3,0]	Yes

For the standard dequantization of Hybrid Encoding, we use Algo. 2 to dequant weights. For example, the (L=4, N=3, S=2) configuration, which is 2.75 bpw, we set weight bit-shift  $\mathbf{W}_{\text{shift}}$  to [4, 2, 0] with 0xF as weight mask  $\mathbf{w}_{\text{mask}}$ ; For the hybrid encoding configuration (L1=3, N1=3, S1=2, L2=3, N2=4, S2=2), we pass  $\mathbf{W}_{\text{shift}}$  with [13, 11, 9, 6, 4, 2, 0] and weight mask  $\mathbf{w}_{\text{mask}}$  with 0x7. As discussed in Section 3.4, we leverage the redundant

---

### Algorithm 2: Dequantization without Code Cluster

---

**Input :**  $\mathbf{W}_{\text{q}}$ : compressed quantized weights  
 $\mathbf{s}_{\text{super}}$ : super scale  
 $\mathbf{zp}$ : weight zero-point  
 $\mathbf{W}_{\text{shift}}$ : bit shift of quantized weight  
 $\mathbf{w}_{\text{mask}}$ : weight mask  
 $\mathbf{s}_{\text{mask}}$ : scale mask  
**Output :**  $\mathbf{W}_{\text{dq}}$ : dequantized weight

```

 $\mathbf{p_w} \leftarrow \text{length of } \mathbf{W}_{\text{shift}}$ ;
 $\mathbf{s}_{\text{uint}} \leftarrow \text{the last value of } \mathbf{W}_{\text{q}}$ ;
 $\mathbf{s} \leftarrow (\mathbf{s}_{\text{uint}} \& \mathbf{s}_{\text{mask}}) \times \mathbf{s}_{\text{super}}$ ;
for each element  $d_w$  in  $\mathbf{W}_{\text{dq}}$  with index  $idx$  do
     $q_w \leftarrow \mathbf{W}_{\text{q}}[idx / \mathbf{p_w}]$ ;
     $w_{\text{uint}} \leftarrow (q_w \gg$ 
         $\mathbf{W}_{\text{shift}}[idx \bmod \mathbf{p_w}]) \& \mathbf{w}_{\text{mask}}$ ;
     $d_w \leftarrow (w_{\text{uint}} - \mathbf{zp}) \times \mathbf{s}$ ;
end

```

---

bits within each weight group to store additional information. During the dequantization process for each computational block, the algorithm efficiently extracts the scaling factors (scale) that are embedded within these redundant bits of the loaded weight matrix  $\mathbf{W}_{\text{q}}$ .

In contrast to the Hybrid Encoding, the encoding configuration (L=6, N=4, S=3) with Code Cluster employs  $\mathbf{W}_{\text{shift}}$  of [9, 6, 3, 0] and  $\mathbf{w}_{\text{mask}}$  of 0x3F, as detailed in Algo. 3. This configuration necessitates two distinct dequantization operations within the main computation loop. The first dequantization operation expands the quantized weights from `UINT8` to `UINT16`, thereby enlarging the numerical space for subsequent processing. The second operation applies different bit-shift operations to dequantize the weights, following a similar approach to Algo. 2. Another key distinction from Algo. 2 stems from the fact that the code cluster eliminates redundant bits entirely, consequently requiring explicit loading of corresponding group-wise quantization scales for each computation block during the main processing loop.

## 4 Experiments

### 4.1 Settings

**Models and Datasets.** We conduct rigorous evaluations using 2 bpw, 2.5 bpw, and 2.75 bpw on two state-of-the-art large language models: DeepSeek-V3-0324 and ERNIE-4.5-300B-A47B. The experiments compare CCQ against 8-bit and 4-bit weight-only quantized models.

We evaluate our model under a unified evaluation protocol across several key benchmarks:

---

**Algorithm 3:** Dequantization with Code Cluster

---

**Input :**  $\mathbf{W}_{\text{q}}$ : compressed quantized weights  
 $s_q$ : quantized scale  
 $s_{\text{super}}$ : super scale  
 $zp$ : weight zero-point  
 $s_{\text{code}}$ : code scale  
 $zp_{\text{code}}$ : code zero-point  
 $\mathbf{W}_{\text{shift}}$ : bit shift of quantized weight  
 $s_{\text{shift}}$ : bit shift of quantized scale  
 $w_{\text{mask}}$ : weight mask  
 $s_{\text{mask}}$ : scale mask

**Output :**  $\mathbf{W}_{\text{dq}}$ : dequantized weight

```

 $s \leftarrow ((s_q \gg s_{\text{shift}}) \& s_{\text{mask}}) \times s_{\text{super}};$ 
 $p_w \leftarrow \text{length of } \mathbf{W}_{\text{shift}};$ 
for each element  $d_w$  in  $\mathbf{W}_{\text{dq}}$  with index  $idx$  do
     $q_w \leftarrow \mathbf{W}_{\text{q}}[idx/p_w];$ 
     $w_{\text{uint}} \leftarrow \text{round}(q_w \times s_{\text{code}} + zp_{\text{code}});$ 
     $w_{\text{uint}} \leftarrow (w_{\text{uint}} \gg s_{\text{shift}});$ 
     $\mathbf{W}_{\text{shift}}[idx \bmod p_w] \& w_{\text{mask}};$ 
     $d_w \leftarrow (w_{\text{uint}} - zp) \times s;$ 
end

```

---

- **Zero-shot** performance on mathematical reasoning (GSM8K (Cobbe et al., 2021)), Chinese mathematics (CMath (Wei et al., 2023)), and multi-step reasoning (MUSR (Sprague et al., 2023)).
- **3-shot** performance on complex task handling (BBH (Srivastava et al., 2022)) and reading comprehension (DROP (Dua et al., 2019)).
- **5-shot** performance on Chinese comprehensive evaluation (C-Eval (Huang et al., 2023)), and massive multi-task language understanding (MMLU (Hendrycks et al., 2021)).

These datasets span critical capabilities including mathematics, reasoning, question answering, reading comprehension, and general tasks. All evaluations use the generation configuration, as per the model’s recommended settings.

**Baselines.** We benchmark our method against 8-bit and 4-bit weight-only quantization. For DeepSeek-V3 (Liu et al., 2024a), comparisons are conducted using open-source quantization models from Hugging Face. For ERNIE 4.5, we adopt Weight-only INT8 (WINT8) as the baseline.

All results across tasks and algorithms are generated under identical evaluation rules. A comprehensive comparison with the aforementioned weight-only quantization approaches is provided in Section 4.2.

## 4.2 Main Results

**Results on DeepSeek-V3.** As summarized in Table 2, our proposed CCQ method achieves comparable performance with mainstream 8-bit and 4-bit weight-only quantization techniques.

While 2-bit RTN weight-only quantization induces a performance cliff with catastrophic accuracy collapse, our 2.06-bit CCQ method reduces memory usage by up to 71.3% from 8-bit models with marginal performance degradation. Section 3.5 provides further hardware-aware optimization analyses.

Table 2: Weight-only quantization results of DeepSeek-V3-0324.

Model Dataset	bpw	DeepSeek-v3-0324				
		Memory	GSM8K	C-Eval	MMLU	Avg
Baseline	8	642GB	96.21	87.31	86.50	90.01
GPTQ <sup>2</sup>	4	346GB	94.77	87.66	86.60	90.04
AWQ <sup>3</sup>	4	328GB	96.13	87.22	86.38	89.43
CCQ (our)	2.75	230GB	95.68	85.08	85.24	88.67
	2.5	212GB	95.60	84.11	85.07	88.26
	2.06	<b>184GB</b>	94.92	84.07	84.29	87.76

**Results on ERNIE 4.5.** As quantified in Table 3, our 2 bpw quantized model reduces GPU memory consumption by 68.33% compared to the WINT8 baseline, while constraining accuracy degradation to around 2%. CCQ establishes a cost-effective inference pathway that enables practical single-GPU deployment on hardware such as NVIDIA H20 devices.

However, on both DeepSeek-V3 and ERNIE 4.5, accuracy drops of CCQ primarily occur in 5-shot C-Eval and MMLU tasks due to instruction-following failures. Future work should focus on improving model adherence to instructions.

## 5 Inference Performance

We conduct comprehensive benchmarks on both individual GEMV (General Matrix-Vector Multiplication) and Grouped-GEMM (Grouped General Matrix-Matrix Multiplication) operators with various matrix shapes and batch size M on the NVIDIA H20 GPU. For GEMV, we compare the performance of VPTQ (Liu et al., 2024b), standard WINT2, and our proposed CCQ implementations

<sup>2</sup>GPTQ:<https://huggingface.co/ISTA-DASLab/DeepSeek-V3-0324-GPTQ-4b-128g-experts>

<sup>3</sup>AWQ:<https://huggingface.co/cognitivecomputations/DeepSeek-V3-0324-AWQ>

Table 3: Weight-only quantization results of ERNIE 4.5.

Model		ERNIE-4.5-300B-A47B							
Dataset	Memory	GSM8K	CMath	MUSR	BBH	DROP	C-Eval	MMLU	Avg
WINT8	281GB	96.6	96.7	69.9	94.3	91.1	90.6	86.5	89.39
WINT4	149GB	96.21	96.5	69.67	94.43	91.17	89.84	86.16	89.14
WINT2	89GB	95.98	96.0	69.57	92.02	89.97	85.39	82.58	87.36

with bpw equal to 2.06. VPTQ is evaluated using its official codebase with recommended inference configurations(bpw=3), while both standard WINT2 and CCQ are implemented with similar Triton-based kernels (Tillet et al., 2019) to ensure a fair comparison. For Grouped-GEMM, we port the CCQ algorithm to the vLLM (Kwon et al., 2023) wna16 operator, a widely adopted Group-GEMM kernel for MoE inference. The baselines (W8A16, W4A16) are experimented on the vLLM library. The key distinction of CCQ lies in its use of two separate dequantization operations per computation block, as well as distinct bit shift configurations.

As shown in Table 4 and Table 5, our CCQ-based implementation consistently delivers superior inference efficiency compared to both traditional and state-of-the-art quantization baselines. In GEMV scenarios, CCQ achieves up to a  $2\times$  speedup over VPTQ and closely matches the performance of standard WINT2, demonstrating that our codebook-free, bit-shift-based dequantization design effectively eliminates the memory access bottlenecks inherent to vector quantization. In Grouped-GEMM settings, which are critical for large-scale MoE inference, CCQ (W2A16-CCQ) not only outperforms widely adopted low-bit operators such as W8A16 and W4A16, but also maintains its latency advantage as batch size and matrix dimensions increase. This scalability underscores the practical value of CCQ for real-world LLM deployment, where both memory footprint and inference speed are crucial. Overall, the results validate that CCQ’s hardware-friendly encoding and decoding pipeline enables highly efficient, large-scale inference without sacrificing model accuracy, making it a compelling solution for low-bit LLM quantization.

## 6 Conclusion

In this study, we propose **convolutional code quantization (CCQ)** to address the inference limitations inherent in vector quantization. By integrating convolutional codes with scalar quantization, we construct a lookup-free encoding space that

Table 4: Operator-level performance comparison on GEMV kernels (execution time in milliseconds).

Matrix Shape Input Size $\times$ Output Size	VPTQ	WINT2-Standard	CCQ
$4096 \times 4096$ (M=1)	0.058	0.027	0.034
$4096 \times 1024$ (M=1)	0.033	0.015	0.017
$8192 \times 8192$ (M=1)	0.174	0.073	0.090
$8192 \times 1024$ (M=1)	0.061	0.019	0.022
$4096 \times 4096$ (M=4)	0.205	0.028	0.035
$4096 \times 1024$ (M=4)	0.112	0.015	0.017
$8192 \times 8192$ (M=4)	0.641	0.076	0.104
$8192 \times 1024$ (M=4)	0.216	0.019	0.024

Table 5: Operator-level performance comparison on Grouped-GEMM kernels (execution time in milliseconds).

Matrix Shape Groups $\times$ Output Size $\times$ Input Size	W8A16	W4A16	W2A16-CCQ
$256 \times 7168 \times 512$ (M=1)	0.044	0.030	0.021
$256 \times 1024 \times 7168$ (M=1)	0.100	0.068	0.058
$256 \times 7168 \times 512$ (M=4)	0.053	0.035	0.027
$256 \times 1024 \times 7168$ (M=4)	0.315	0.199	0.166
$256 \times 7168 \times 512$ (M=16)	0.104	0.071	0.059
$256 \times 1024 \times 7168$ (M=16)	1.052	0.624	0.527
$256 \times 7168 \times 512$ (M=64)	0.297	0.193	0.161
$256 \times 1024 \times 7168$ (M=64)	2.655	1.628	1.386

achieves a linear mapping between the codebook and weight vectors, thereby optimizing inference performance. Meanwhile, by maintaining high-bit quantization precision for weights, we minimize the performance degradation of the model under extremely low-bit conditions. Through the introduction of hybrid encoding, we can flexibly apply coding quantization to improve the compression ratio. Furthermore, by leveraging the characteristic of normal distribution of convolutional code values across weights, we propose Code Cluster to reduce redundancy in the encoding space. Ultimately, we expand the encoding configurations of CCQ, which not only enhances model accuracy but also further compresses the model size.

## 7 Future Work

In the domain of extreme low-bit quantization, we identify loss-based dynamic bit allocation as a critical research direction. For instance, during ERNIE 4.5 quantization, we observe that allocating only the 6th MoE layer as WINT4 (instead of CCQ) could maintain high accuracy, while the other expert layers retained CCQ with bpw equal to 2.06. This finding prompts us to ponder whether certain individual layers in LLMs play a pivotal role in preserving the model’s capabilities. Meanwhile, our proposed algorithmic framework for encode quantization can theoretically be extended to other coding theories, demonstrating significant scalability. This will also be one of the key directions for our future exploration. While our experiments validate the efficacy on the MoE architecture, further investigation is warranted for dense models under state-of-the-art 2-bit quantization methods such as QTIP (Tseng et al., 2024b) and VPTQ (Liu et al., 2024b). Additionally, inference kernel optimization presents substantial headroom through joint consideration of permutation strategies during both quantization and runtime execution. Co-designing these phases could yield latency reductions, particularly for memory-bound operations on devices.

## References

Hicham Badri and Appu Shaji. 2023. [Half-quadratic quantization of large machine learning models](#).

Hicham Badri and Appu Shaji. 2024. [Towards 1-bit machine learning models](#).

Baidu-ERNIE-Team. 2025. Ernie 4.5 technical report.

Karl Cobbe, Vineet Kosaraju, Mohammad Bavarian, Mark Chen, Heewoo Jun, Lukasz Kaiser, Matthias Plappert, Jerry Tworek, Jacob Hilton, Reiichiro Nakano, et al. 2021. Training verifiers to solve math word problems. *arXiv preprint arXiv:2110.14168*.

DeepSeek-AI, Aixin Liu, Bei Feng, and et.al. 2025. [Deepseek-v3 technical report](#). *Preprint, arXiv:2412.19437*.

Dheeru Dua, Yizhong Wang, Pradeep Dasigi, Gabriel Stanovsky, Sameer Singh, and Matt Gardner. 2019. Drop: A reading comprehension benchmark requiring discrete reasoning over paragraphs. *arXiv preprint arXiv:1903.00161*.

Vage Egiazarian, Andrei Panferov, Denis Kuznedelev, Elias Frantar, Artem Babenko, and Dan Alistarh. 2024. [Extreme compression of large language models via additive quantization](#). *Preprint, arXiv:2401.06118*.

Elias Frantar, Saleh Ashkboos, Torsten Hoefer, and Dan Alistarh. 2022. Gptq: Accurate post-training quantization for generative pre-trained transformers. *arXiv preprint arXiv:2210.17323*.

Aaron Grattafiori, Abhimanyu Dubey, and et.al. 2024. [The llama 3 herd of models](#). *Preprint, arXiv:2407.21783*.

Robert Gray. 1984. Vector quantization. *IEEE Assp Magazine*, 1(2):4–29.

Robert M. Gray and David L. Neuhoff. 1998. Quantization. *IEEE transactions on information theory*, 44(6):2325–2383.

Dan Hendrycks, Collin Burns, Steven Basart, Andy Zou, Mantas Mazeika, Dawn Song, and Jacob Steinhardt. 2021. Measuring massive multitask language understanding. *Proceedings of the International Conference on Learning Representations (ICLR)*.

Coleman Hooper, Sehoon Kim, Hiva Mohammadzadeh, Michael W Mahoney, Yakun S Shao, Kurt Keutzer, and Amir Gholami. 2024. Kvquant: Towards 10 million context length llm inference with kv cache quantization. *Advances in Neural Information Processing Systems*, 37:1270–1303.

Yuzhen Huang, Yuzhuo Bai, Zhihao Zhu, Junlei Zhang, Jinghan Zhang, Tangjun Su, Junteng Liu, Chuancheng Lv, Yikai Zhang, Jiayi Lei, Yao Fu, Maosong Sun, and Junxian He. 2023. C-eval: A multi-level multi-discipline chinese evaluation suite for foundation models. In *Advances in Neural Information Processing Systems*.

Sehoon Kim, Coleman Hooper, Amir Gholami, Zhen Dong, Xiuyu Li, Sheng Shen, Michael W Mahoney, and Kurt Keutzer. 2023. Squeezellm: Dense-and-sparse quantization. *arXiv preprint arXiv:2306.07629*.

Woosuk Kwon, Zhuohan Li, Siyuan Zhuang, Ying Sheng, Lianmin Zheng, Cody Hao Yu, Joseph E. Gonzalez, Hao Zhang, and Ion Stoica. 2023. Efficient memory management for large language model serving with pagedattention. In *Proceedings of the ACM SIGOPS 29th Symposium on Operating Systems Principles*.

Banseok Lee, Dongkyu Kim, Youngcheon You, and Youngmin Kim. 2025. [Littlebit: Ultra low-bit quantization via latent factorization](#). *Preprint, arXiv:2506.13771*.

Yuhang Li, Ruokai Yin, Donghyun Lee, Shiting Xiao, and Priyadarshini Panda. 2025. Gptaq: Efficient finetuning-free quantization for asymmetric calibration. *arXiv preprint arXiv:2504.02692*.

Ji Lin, Jiaming Tang, Haotian Tang, Shang Yang, Wei-Ming Chen, Wei-Chen Wang, Guangxuan Xiao, Xingyu Dang, Chuang Gan, and Song Han. 2024. Awq: Activation-aware weight quantization for on-device llm compression and acceleration. *Proceedings of Machine Learning and Systems*, 6:87–100.

Aixin Liu, Bei Feng, Bing Xue, Bingxuan Wang, Bochao Wu, Chengda Lu, Chenggang Zhao, Chengqi Deng, Chenyu Zhang, Chong Ruan, et al. 2024a. Deepseek-v3 technical report. *arXiv preprint arXiv:2412.19437*.

Yifei Liu, Jicheng Wen, Yang Wang, Shengyu Ye, Li Lyra Zhang, Ting Cao, Cheng Li, and Mao Yang. 2024b. Vptq: Extreme low-bit vector post-training quantization for large language models. *arXiv preprint arXiv:2409.17066*.

Zechun Liu, Barlas Oguz, Changsheng Zhao, Ernie Chang, Pierre Stock, Yashar Mehdad, Yangyang Shi, Raghuraman Krishnamoorthi, and Vikas Chandra. 2023. Llm-qat: Data-free quantization aware training for large language models. *arXiv preprint arXiv:2305.17888*.

Zirui Liu, Jiayi Yuan, Hongye Jin, Shaochen Zhong, Zhaozhuo Xu, Vladimir Braverman, Beidi Chen, and Xia Hu. 2024c. Kivi: A tuning-free asymmetric 2bit quantization for kv cache. *arXiv preprint arXiv:2402.02750*.

Vladimir Malinovskii, Denis Mazur, Ivan Ilin, Denis Kuznedelev, Konstantin Burlachenko, Kai Yi, Dan Alistarh, and Peter Richtarik. 2024. Pv-tuning: Beyond straight-through estimation for extreme llm compression. *Preprint, arXiv:2405.14852*.

Michael W Marcellin and Thomas R Fischer. 1990. Trellis coded quantization of memoryless and gauss-markov sources. *IEEE transactions on communications*, 38(1):82–93.

Zayne Sprague, Xi Ye, Kaj Bostrom, Swarat Chaudhuri, and Greg Durrett. 2023. Musr: Testing the limits of chain-of-thought with multistep soft reasoning. *arXiv preprint arXiv:2310.16049*.

Aarohi Srivastava, Abhinav Rastogi, Abhishek Rao, Abu Awal Md Shoeb, Abubakar Abid, Adam Fisch, Adam R Brown, Adam Santoro, Aditya Gupta, Adrià Garriga-Alonso, et al. 2022. Beyond the imitation game: Quantifying and extrapolating the capabilities of language models. *arXiv preprint arXiv:2206.04615*.

Philippe Tillet, Hsiang-Tsung Kung, and David Cox. 2019. Triton: an intermediate language and compiler for tiled neural network computations. In *Proceedings of the 3rd ACM SIGPLAN International Workshop on Machine Learning and Programming Languages*, pages 10–19.

Albert Tseng, Jerry Chee, Qingyao Sun, Volodymyr Kuleshov, and Christopher De Sa. 2024a. Quip#: Even better llm quantization with hadamard incoherence and lattice codebooks. *arXiv preprint arXiv:2402.04396*.

Albert Tseng, Qingyao Sun, David Hou, and Christopher M De Sa. 2024b. Qtip: Quantization with trellises and incoherence processing. *Advances in Neural Information Processing Systems*, 37:59597–59620.

Mart van Baalen, Andrey Kuzmin, Markus Nagel, Peter Couperus, Cedric Bastoul, Eric Mahurin, Tijmen Blankevoort, and Paul Whatmough. 2024. Gptvq: The blessing of dimensionality in llm quantization. *arXiv preprint arXiv:2402.15319*.

Hongyu Wang, Shuming Ma, Li Dong, Shaohan Huang, Huaijie Wang, Lingxiao Ma, Fan Yang, Ruiping Wang, Yi Wu, and Furu Wei. 2023. Bitnet: Scaling 1-bit transformers for large language models. *arXiv preprint arXiv:2310.11453*.

Tianwen Wei, Jian Luan, Wei Liu, Shuang Dong, and Bin Wang. 2023. Cmath: Can your language model pass chinese elementary school math test? *arXiv preprint arXiv:2306.16636*.

Guangxuan Xiao, Ji Lin, Mickael Seznec, Hao Wu, Julien Demouth, and Song Han. 2023. Smoothquant: Accurate and efficient post-training quantization for large language models. In *International Conference on Machine Learning*, pages 38087–38099. PMLR.

Yuzhuang Xu, Xu Han, Zonghan Yang, Shuo Wang, Qingfu Zhu, Zhiyuan Liu, Weidong Liu, and Wanxiang Che. 2024. Onebit: Towards extremely low-bit large language models. *Preprint, arXiv:2402.11295*.

An Yang, Anfeng Li, Baosong Yang, Beichen Zhang, Binyuan Hui, Bo Zheng, Bowen Yu, Chang Gao, Chengan Huang, Chenxu Lv, Chujie Zheng, Dayiheng Liu, Fan Zhou, Fei Huang, Feng Hu, Hao Ge, Haoran Wei, Huan Lin, Jialong Tang, Jian Yang, Jianhong Tu, Jianwei Zhang, Jianxin Yang, Jiaxi Yang, Jing Zhou, Jingren Zhou, Junyang Lin, Kai Dang, Keqin Bao, Kexin Yang, Le Yu, Lianghao Deng, Mei Li, Mingfeng Xue, Mingze Li, Pei Zhang, Peng Wang, Qin Zhu, Rui Men, Ruize Gao, Shixuan Liu, Shuang Luo, Tianhao Li, Tianyi Tang, Wenbiao Yin, Xingzhang Ren, Xinyu Wang, Xinyu Zhang, Xuancheng Ren, Yang Fan, Yang Su, Yichang Zhang, Yinger Zhang, Yu Wan, Yuqiong Liu, Zekun Wang, Zeyu Cui, Zhenru Zhang, Zhipeng Zhou, and Zihan Qiu. 2025. Qwen3 technical report. *arXiv preprint arXiv:2505.09388*.

An Yang, Baosong Yang, Binyuan Hui, Bo Zheng, Bowen Yu, Chang Zhou, Chengpeng Li, Chengyuan Li, Dayiheng Liu, Fei Huang, Guanting Dong, Haoran Wei, Huan Lin, Jialong Tang, Jialin Wang, Jian Yang, Jianhong Tu, Jianwei Zhang, Jianxin Ma, Jin Xu, Jingren Zhou, Jinze Bai, Jinzheng He, Junyang Lin, Kai Dang, Keming Lu, Keqin Chen, Kexin Yang, Mei Li, Mingfeng Xue, Na Ni, Pei Zhang, Peng Wang, Ru Peng, Rui Men, Ruize Gao, Runji Lin, Shijie Wang, and et.al. 2024a. Qwen2 technical report. *arXiv preprint arXiv:2407.10671*.

An Yang, Baosong Yang, Beichen Zhang, Binyuan Hui, Bo Zheng, Bowen Yu, Chengyuan Li, Dayiheng Liu, Fei Huang, Haoran Wei, Huan Lin, Jian Yang, Jianhong Tu, Jianwei Zhang, Jianxin Yang, Jiaxi Yang, Jingren Zhou, Junyang Lin, Kai Dang, Keming Lu, Keqin Bao, Kexin Yang, Le Yu, Mei Li, Mingfeng Xue, Pei Zhang, Qin Zhu, and et.al. 2024b. Qwen2.5 technical report. *arXiv preprint arXiv:2412.15115*.